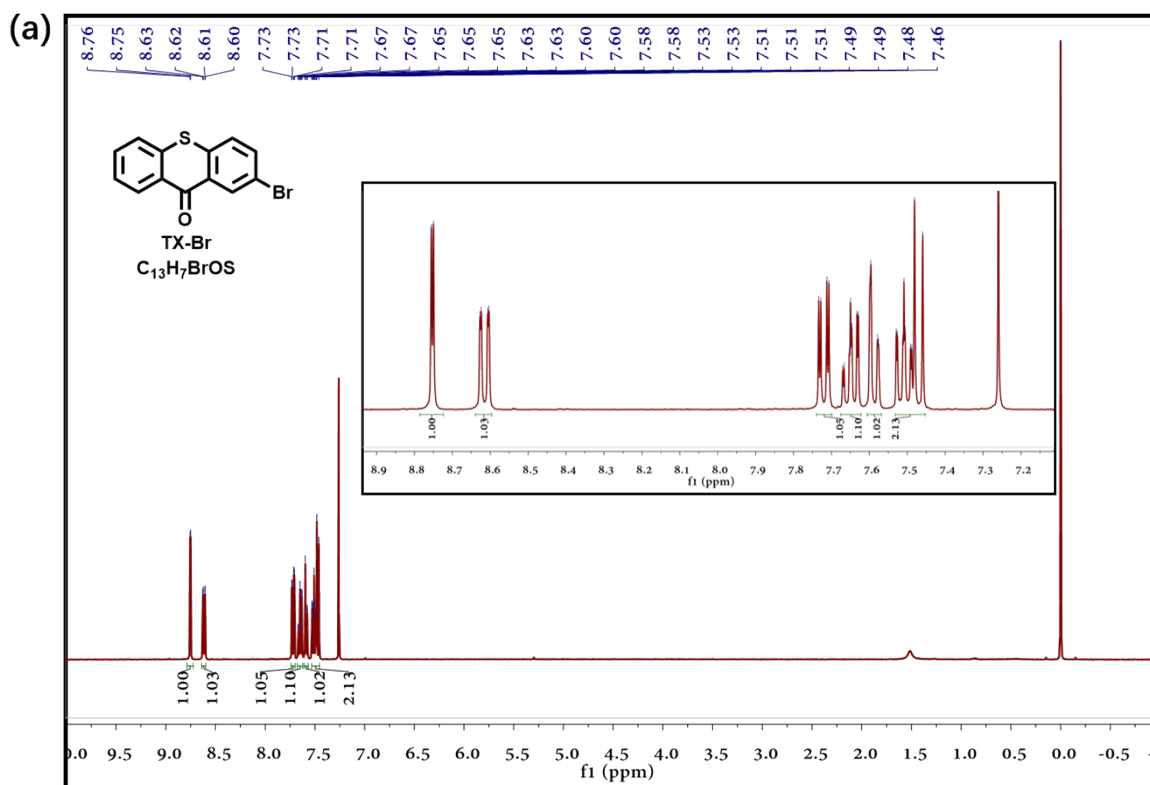


## Supporting Information

### Highly Efficient Purely Organic Room-Temperature Phosphorescence Film based on a Selenium-Containing Emitter for Sensitive Oxygen Detection

Shuai Wang, Haiyang Shu, Xianchao Han, Xiaofu Wu, Hui Tong\*, Lixiang Wang\*

#### 1. Experimental details



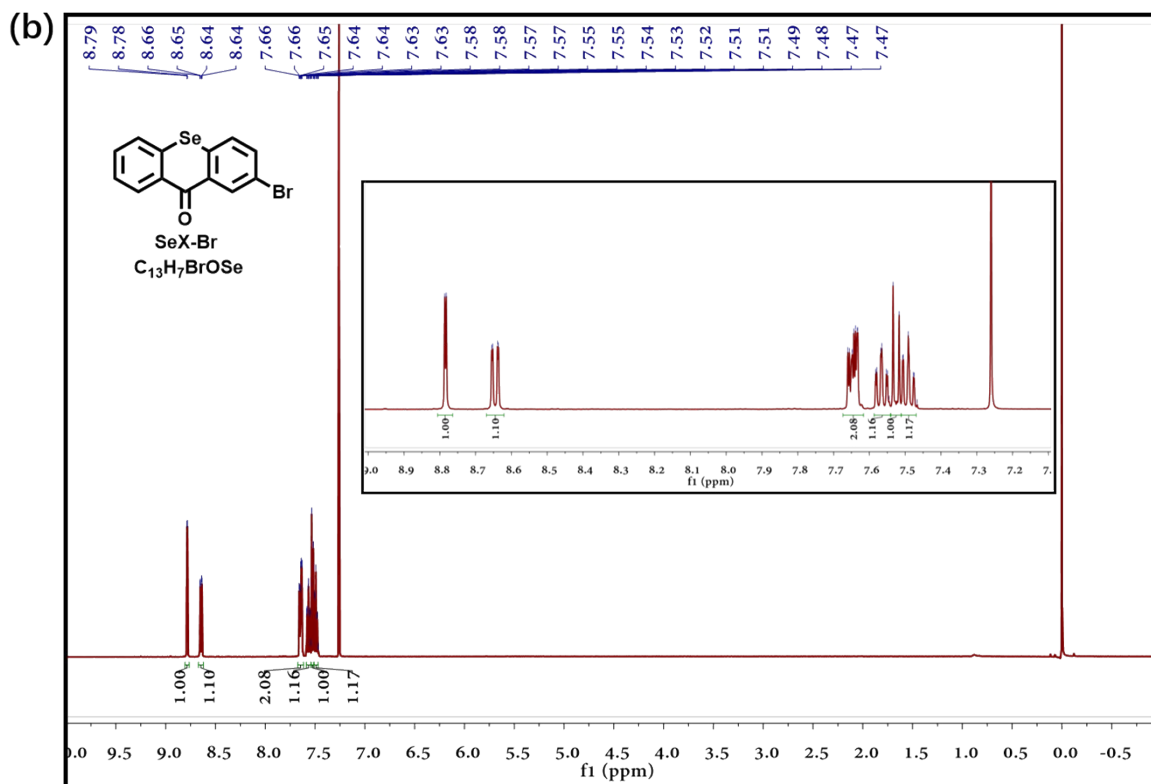
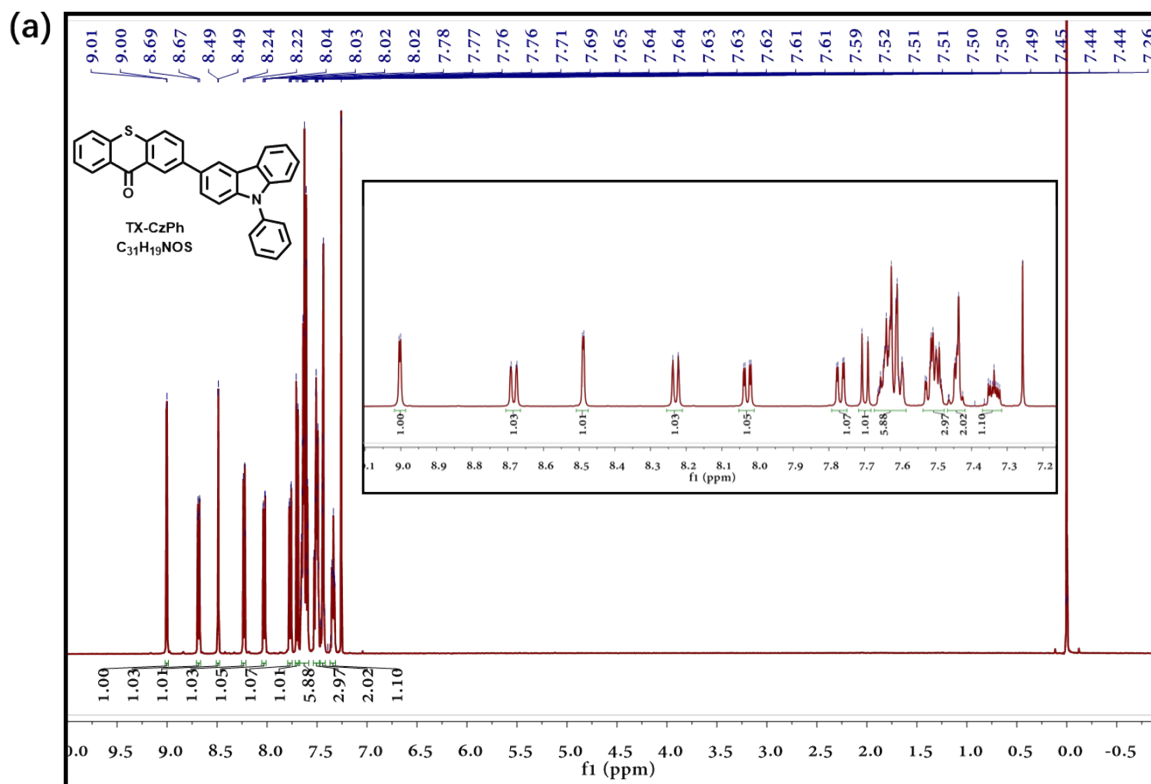


Figure S1.  $^1H$  NMR of TX-Br (a) and SeX-Br (b)



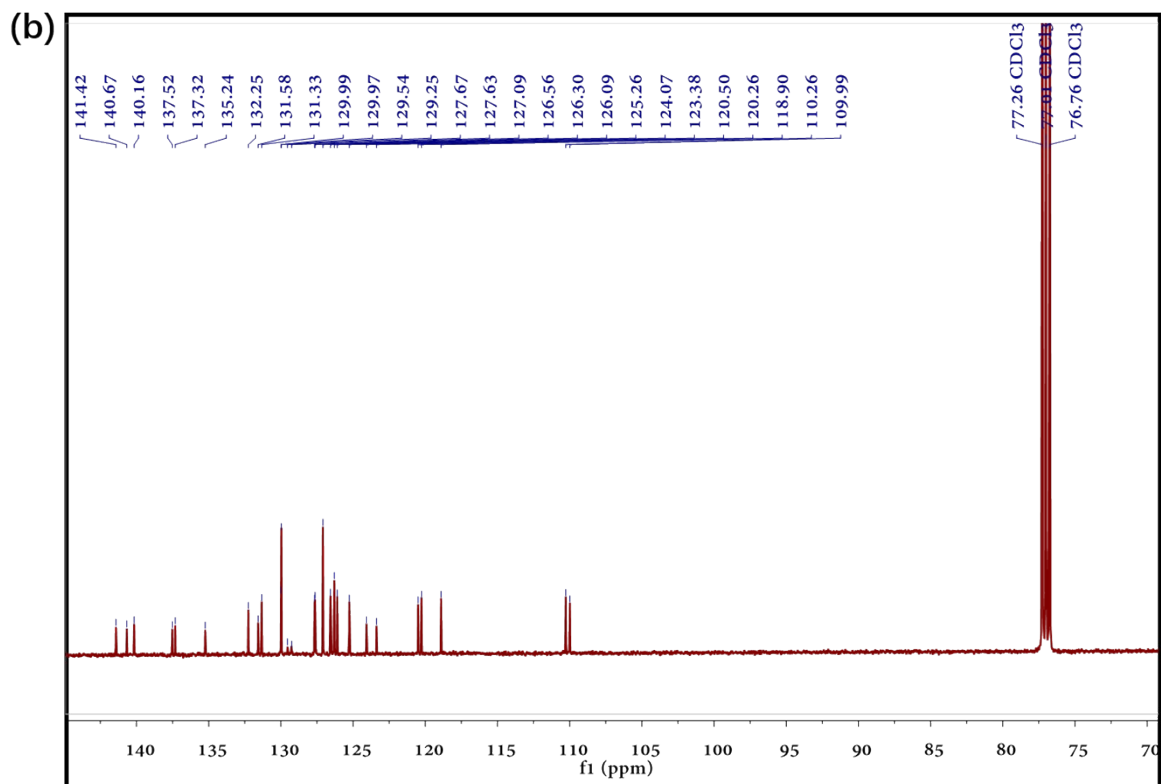
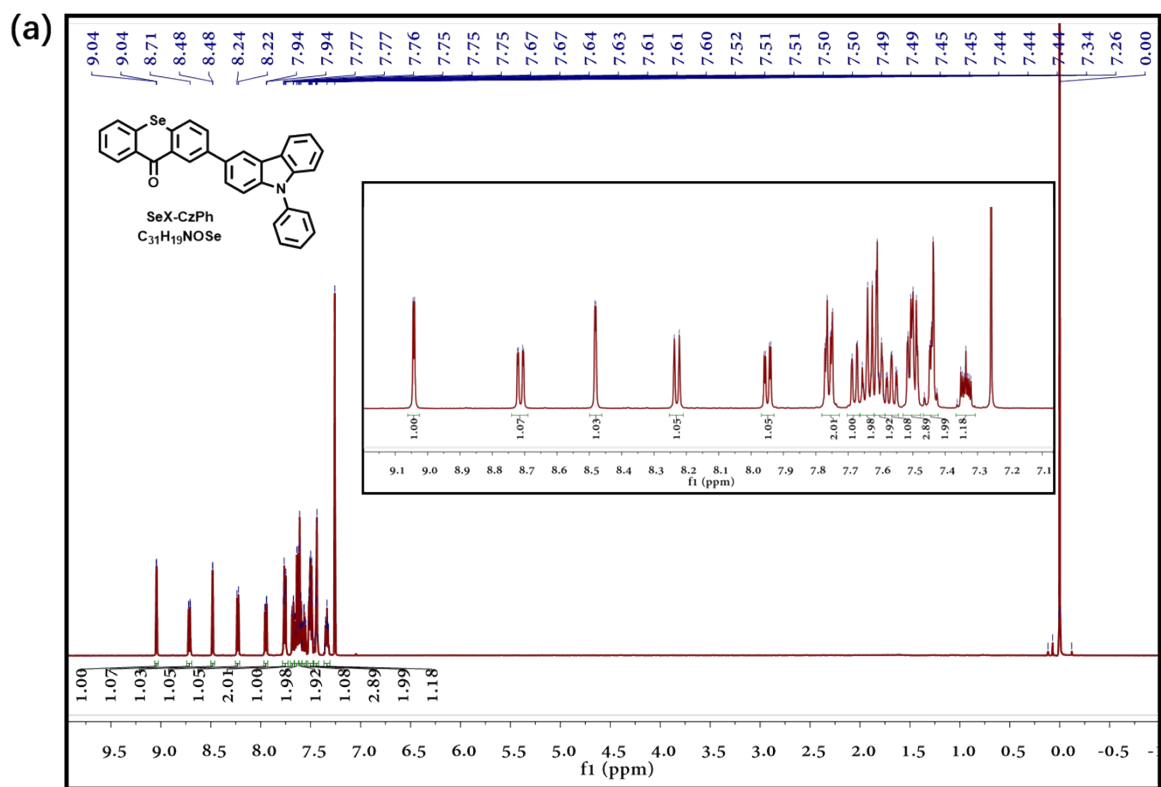


Figure S2. <sup>1</sup>H NMR (a) and <sup>13</sup>C NMR (b) of TX-CzPh



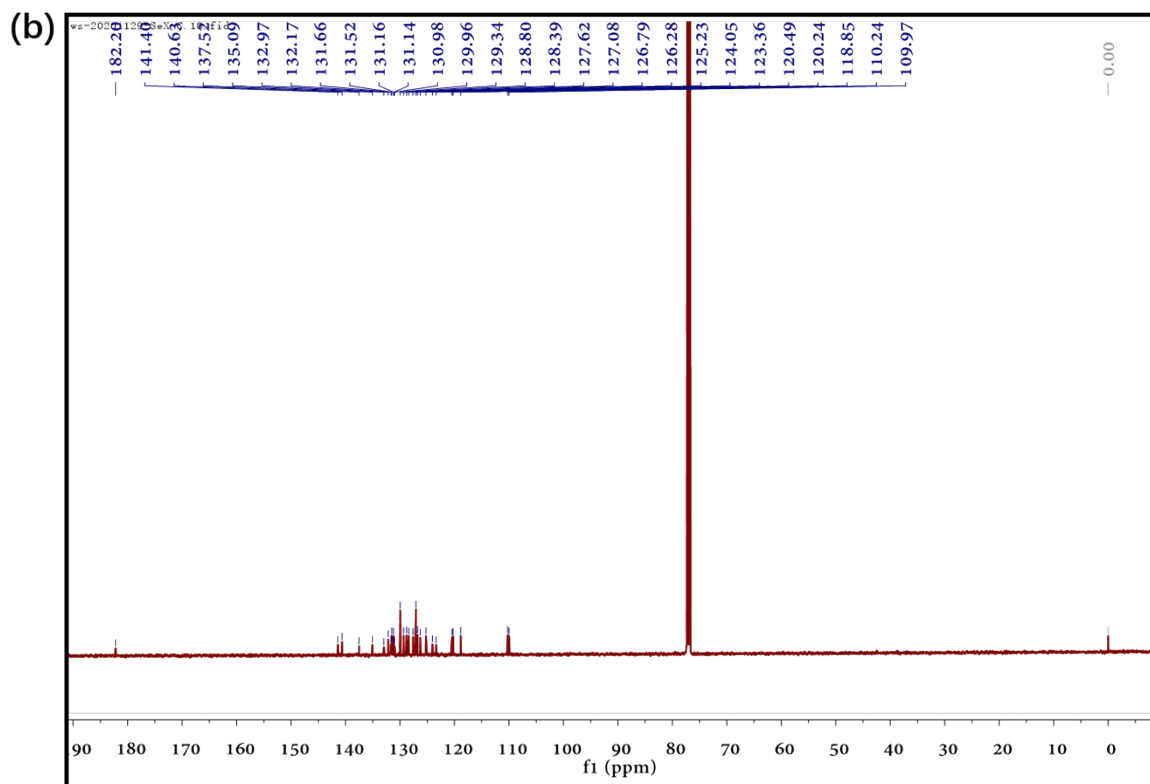


Figure S3.  $^1\text{H}$  NMR (a) and  $^{13}\text{C}$  NMR (b) of SeX-CzPh

## 2. Photophysical measurements

The radiative rate constants of fluorescence ( $k_r^F$ ), phosphorescence ( $k_r^P$ ), the intersystem crossing rate constant ( $k_{ISC}$ ), and the sum of the nonradiative constant of phosphorescence ( $k_{nr}^P$ ) and quenching rate of T<sub>1</sub> ( $k_q$ ) of SeX-CzPh and TX-CzPh were calculated according to the following equations:

$$\Phi_{FL} = 1 - \Phi_{ISC} - \Phi_{nr}^F \quad (S1)$$

$$\Phi_{Ph} = \Phi_{ISC} - \Phi_{nr}^P - \Phi_q \quad (S2)$$

$$k_r^F = \frac{\Phi_{FL}}{\tau_{FL}} \quad (S3)$$

$$k_{ISC} = \frac{\Phi_{ISC}}{\tau_{FL}} \quad (S4)$$

$$\frac{1}{\tau_{FL}} = k_r^F + k_{nr}^F + k_{ISC} \quad (S5)$$

$$\Phi_{FL} = \frac{k_r^F}{k_r^F + k_{nr}^F + k_{ISC}} \quad (S6)$$

$$\frac{1}{\tau_{Ph}} = k_r^P + k_{nr}^P + k_q \quad (S7)$$

$$\Phi_{Ph} = \frac{\Phi_{ISC} k_r^P}{k_r^P + k_{nr}^P + k_q} \quad (S8)$$

where  $\Phi_{FL}$ ,  $\Phi_{Ph}$  and  $\Phi_{ISC}$  are the absolute quantum yield of fluorescence, phosphorescence and intersystem crossing, and  $\Phi_{nr}^F$  and  $\Phi_{nr}^P$  is the nonradiative absolute quantum yield of fluorescence and phosphorescence, and  $k_q$  is the quenching absolute quantum yield of T<sub>1</sub>, and  $\tau_{FL}$  and  $\tau_{Ph}$  are the average lifetime of fluorescence and phosphorescence, and  $k_{nr}^F$  is the nonradiative constant of fluorescence. The quantum yield of the intersystem crossing ( $\Phi_{ISC}$ ) could be assumed to be  $1 - \Phi_{FL}$  according to the following equations (S1) and (S2), since both SeX-CzPh and TX-CzPh showed intense phosphorescence emission with negligible fluorescence emission in 2-methyltetrahydrofuran solutions at 77 K.<sup>1-2, 5</sup>

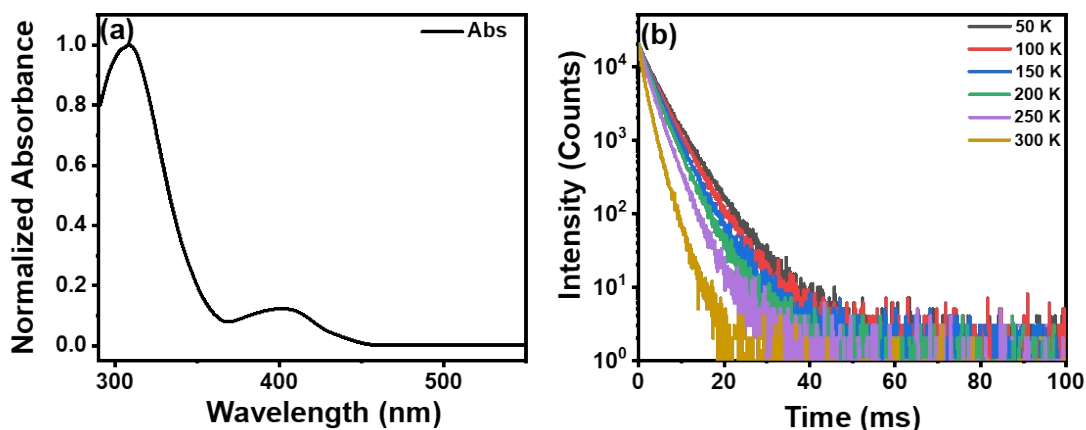


**Figure S4.** (a) UV-vis spectra of SeX-CzPh in toluene and (b) temperature-dependent time-resolved PL decay spectra of SeX-CzPh doped film at 500 nm.

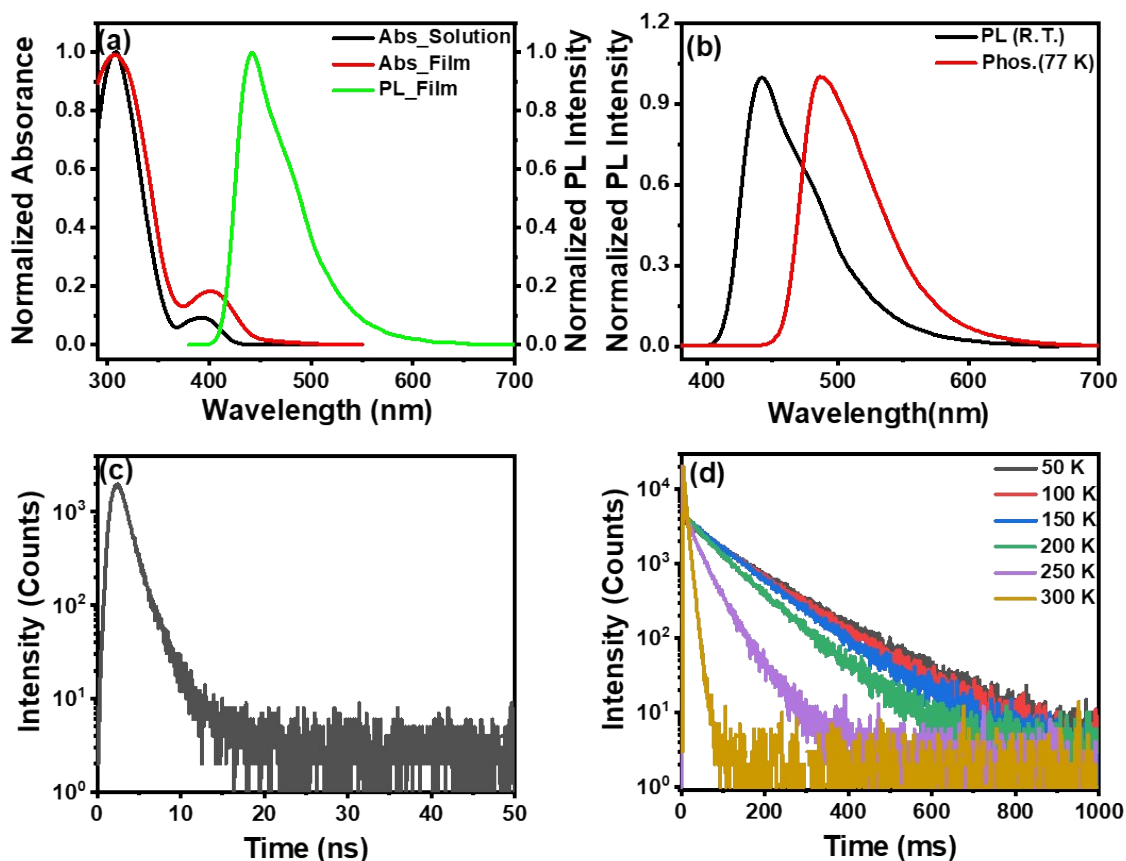


**Figure S5.** (a) UV-vis spectra of TX-CzPh in toluene (black) and doped film (red) and steady-state PL spectra of TX-CzPh doped film (green) at room temperature; (b) steady-state PL (black) at room temperature and delay spectra (red) at 77 K (delay time: 1 ms) of TX-CzPh doped film; (c) time-resolved PL decay spectra measured at 441 nm of TX-CzPh doped film at room temperature; (d) temperature-dependent time-resolved PL decay spectra of TX-CzPh doped film at 487 nm.

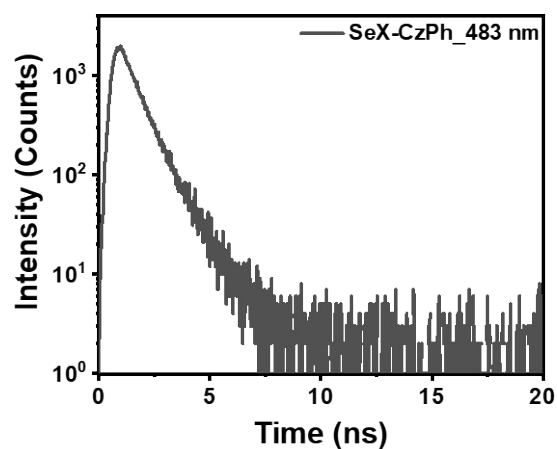


**Figure S6.** Time-resolved PL decay spectra measured at 483 nm of SeX-CzPh crystal powder at room temperature

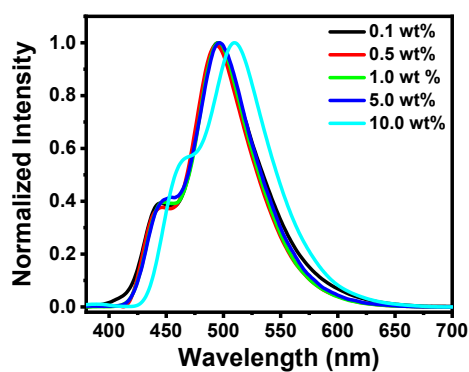


**Figure S7.** Steady-state PL spectra of SeX-CzPh doped film with different doping concentrations

The PLQY of 0.1 wt%, 0.5 wt%, 1 wt%, 5 wt% and 10 wt% SeX-CzPh doped films in vacuum at room temperature are 47.9%, 47.6%, 48.1%, 46.9% and 39.8%, respectively.

**Table S1.** Summary of phosphorescent quantum yields of organic RTP materials doped films

Compound	Host	$\lambda_{\text{PL}}$ [nm]	$\Phi_{\text{Ph}}$ [%]	Ref
DPTZ-DBT	Zeonex	540	60	1
4	$\beta$ -estradiol	550	50	2
<b>SeX-CzPh</b>	<b>PS</b>	<b>500</b>	<b>44.3</b>	<b>This work</b>
HTO	PVA	467	44	3
2a	Zeonex	554	39.5	4
PSe2	DPEPO	500	35	5
PVA-100-2-HC-1	PVA	470	29.2	6
<b>TX-CzPh</b>	<b>PS</b>	<b>487</b>	<b>10.1</b>	<b>This work</b>
I-BF2dbm-OCH3	PMMA	517	4.5	7
TXCl	PMMA	487	0.95	8



**Table S2.** Summary of the photophysical properties of SeX-CzPh and TX-CzPh

	State	$\lambda_{\text{PL}}$ [nm]	$\Phi_{\text{PL}}$ [%]	$\Phi_{\text{FL}}$ [%]	$\Phi_{\text{Ph}}$ [%]	$\tau_{\text{FL}}$ [ns]	$\tau_{\text{ph}}$ [ms]	$k_r^F$ [ $10^7 \text{ s}^{-1}$ ]	$k_{\text{ISC}}$ [ $10^8 \text{ s}^{-1}$ ]	$k_r^P$ [ $10^2 \text{ s}^{-1}$ ]	$k_{nr} + k_q$ [ $10^3 \text{ s}^{-1}$ ]
SeX-CzPh	Doped Film	453, 500	48.1	3.8	44.3	1.08	1.62	3.5	8.9	2.8	0.3
	Crystal Powder	481, 544	5.0	2.1	2.9	0.79	0.016	2.6	12.4	18.9	61.7
TX-CzPh	Doped Film	441, 487	21.9	11.8	10.1	1.35	10.35	8.7	6.5	0.1	0.9
	Crystal Powder	472, 529	29.3	7.6	21.7	1.21	0.61	6.3	7.7	3.9	1.3

**Table S3** Photophysical properties of TX-CzPh and SeX-CzPh

	TX-CzPh <sup>a</sup>		SeX-CzPh <sup>a</sup>		SeX-CzPh <sup>b</sup>	
$\lambda_{\text{em}}$	441 nm	487 nm	451 nm	500 nm	483 nm	543 nm
$\tau_{\text{avg}}$	1.35 ns	10.31 ms	1.08 ns	1.65 ms	0.79 ns	15.74 $\mu\text{s}$
$\tau_1$		1.88 ms (8.2 %)		0.07 ms (3.4 %)		15.24 $\mu\text{s}$ (99.5%)
$\tau_2$		7.76 ms (53.5 %)		0.86 ms (34.4 %)		533.12 $\mu\text{s}$ (0.5%)
$\tau_3$		15.71 ms (38.3 %)		2.12 ms (62.2 %)		

<sup>a</sup> doped film. <sup>b</sup> crystal powder

### 3. Oxygen Sensing

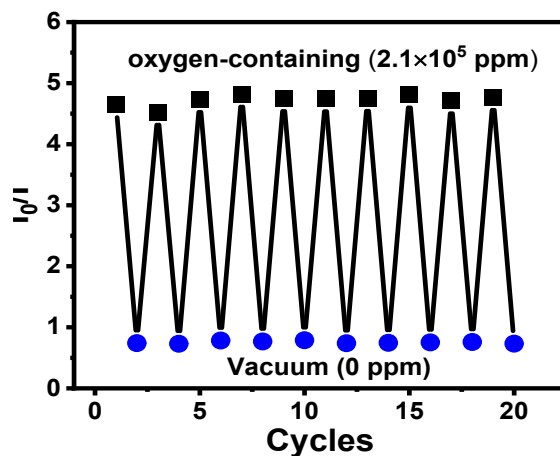


**Figure S8.** Reversible oxygen response of the TX-CzPh doped film

**Table S4.** Summary of the oxygen sensing properties of some phosphorescent materials

Probe	Linear [10 <sup>4</sup> ppm]	$K_{SV} \times 10^{-4}$ [ppm <sup>-1</sup> ]	LOD <sup>a</sup> [ppm]	R <sup>2</sup>	Test method	Ref
SeX-CzPh	0-21	1.27	4.9	0.997	PL Intensity	This work
TX-CzPh	0-4	1.08	10.7	0.994	PL Intensity	This work
TBBU	0-21	1.26	5.0	0.998	Lifetime	9
SNPs	0-3	1.92	3.3	0.994	PL Intensity	10
2FT	0-0.3	5.32	1.2	0.999	PL Intensity	11
4FT	0-0.3	4.04	1.6	0.977	PL Intensity	
Lu-DVDMS	0-1	0.062	100.4	-	PL Intensity	12
Cu(POP)phencarz]- BF4-PS	0-100	0.15	41.7	0.997	PL Intensity	13
Pd-Al LDHs/Pd- TCPP	0-100	0.008	777.9	0.972	PL Intensity	14

#### 4. X-ray crystallographic analysis

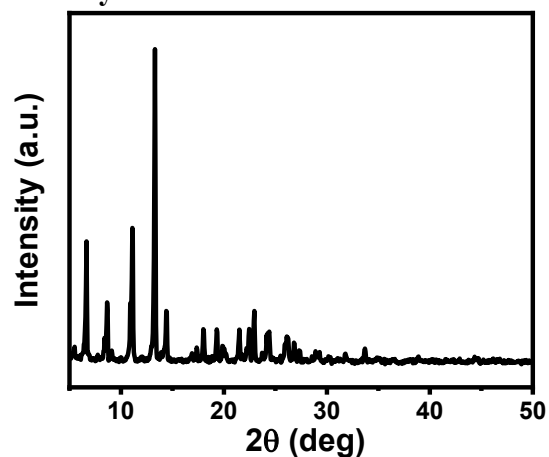
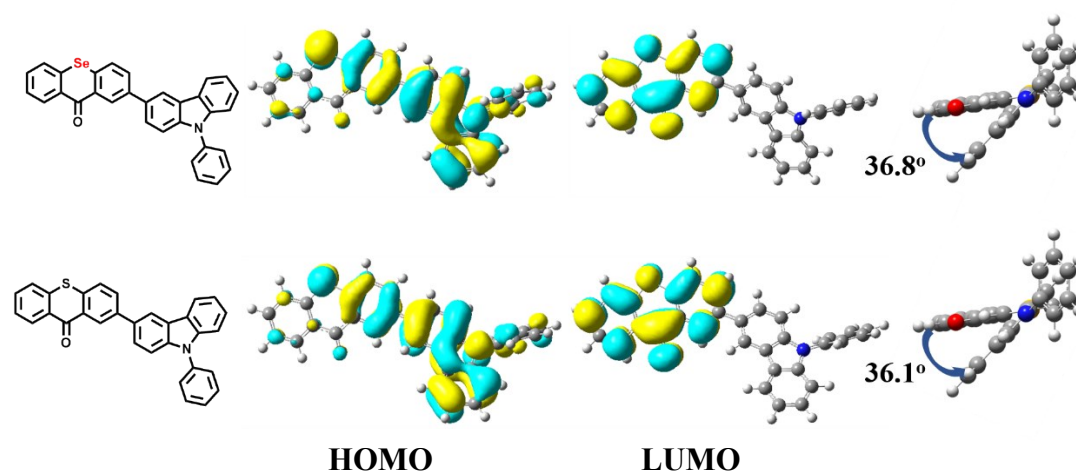


Figure S9. Powder X-ray diffraction patterns of SeX-CzPh crystal powder

Table S5. Single crystal Data of SeX-CzPh

Name	SeX-CzPh	
Empirical formula	C <sub>31</sub> H <sub>19</sub> NOSe	
Formula weight	500.43	
Temperature	301(2)	
Crystal system	Monoclinic	
Space group	P21/c	
Unit cell dimensions	a = 4.0113(4)	alpha = 90.00
	b = 20.9812(19)	beta = 94.065
	c = 25.560 (2)	gamma = 90.00
Volume	2145.8(4)	
Z	4	
Density	1.549	
F (000)	1016.0	
Radiation	Mo K $\alpha$ radiation ( $\lambda$ = 0.71073 Å)	
Cell measurement theta min	2.5858	
Cell measurement theta max	27.7594	

## 5. Theoretical calculation results



**Figure S10.** The molecular orbital distributions and the dihedral angles of SeX-CzPh and TX-CzPh

	SeX-CzPh			TX-CzPh			
	Hole	Electron		Hole	Electron		
S <sub>1</sub>		→	(n,π*)	S <sub>1</sub>		→	(n,π*)
T <sub>1</sub>		→	(π,π*)	T <sub>1</sub>		→	(π,π*)
T <sub>2</sub>		→	(π,π*)	T <sub>2</sub>		→	(π,π*)
T <sub>3</sub>		→	(π,π*)	T <sub>3</sub>		→	(π,π*)
T <sub>4</sub>		→	(π,π*)	T <sub>4</sub>		→	(π,π*)
T <sub>5</sub>		→	(π,π*)	T <sub>5</sub>		→	(π,π*)
T <sub>6</sub>		→	(π,π*)	T <sub>6</sub>		→	(π,π*)
T <sub>7</sub>		→	(π,π*)	T <sub>7</sub>		→	(π,π*)
T <sub>8</sub>		→	(π,π*)	T <sub>8</sub>		→	(π,π*)

**Figure S11.** Hole-Electron analysis of SeX-CzPh and TX-CzPh in the lowest single (S<sub>1</sub>) and triplet manifolds (T<sub>n</sub>) base on the geometry of S<sub>1</sub> state.

**Table S6.** Energy levels of SeX-CzPh monomer

<b>Excited state</b>	<b>Energy level (eV)</b>
S <sub>1</sub>	3.7451
T <sub>1</sub>	3.0549
T <sub>2</sub>	3.3635
T <sub>3</sub>	3.4572
T <sub>4</sub>	3.6218
T <sub>5</sub>	3.7397
T <sub>6</sub>	3.7758
T <sub>7</sub>	4.0095
T <sub>8</sub>	4.1093

**Table S7.** SOC constant of SeX-CzPh monomer

	<b>SOC (cm<sup>-1</sup>)</b>
$\zeta_{S_0-T_1}$	4.09
$\zeta_{S_1-T_1}$	52.50
$\zeta_{S_1-T_2}$	3.80
$\zeta_{S_1-T_3}$	13.00
$\zeta_{S_1-T_4}$	0.99
$\zeta_{S_1-T_5}$	8.48
$\zeta_{S_1-T_6}$	4.17
$\zeta_{S_1-T_7}$	2.02
$\zeta_{S_1-T_8}$	14.20

**Table S8.** Energy levels of TX-CzPh monomer

<b>Excited state</b>	<b>Energy level (eV)</b>
S <sub>1</sub>	3.7819
T <sub>1</sub>	3.1064
T <sub>2</sub>	3.4025
T <sub>3</sub>	3.4349
T <sub>4</sub>	3.6208
T <sub>5</sub>	3.7325
T <sub>6</sub>	3.7957
T <sub>7</sub>	4.0135
T <sub>8</sub>	4.1332

**Table S9.** SOC constant of TX-CzPh monomer

	<b>SOC (cm<sup>-1</sup>)</b>
$\zeta_{S_0-T_1}$	1.33
$\zeta_{S_1-T_1}$	26.19
$\zeta_{S_1-T_2}$	2.02
$\zeta_{S_1-T_3}$	4.47
$\zeta_{S_1-T_4}$	2.23
$\zeta_{S_1-T_5}$	7.87
$\zeta_{S_1-T_6}$	11.01
$\zeta_{S_1-T_7}$	3.04
$\zeta_{S_1-T_8}$	9.78

## Reference

- 1 R. Huang, J. S. Ward, N. A. Kukhta, J. Avó, J. Gibson, T. Penfold, J. C. Lima, A. S. Batsanov, M. N. Berberan-Santos, M. R. Bryce, and F. B. Dias, *J. Mater. Chem. C*, 2018, **6**, 9238-9248.
- 2 I. Bhattacharjee, and S. Hirata, *Adv. Mater.*, 2020, **32**, 2001348.
- 3 L. Ma, S. Sun, B. Ding, X. Ma, and H. Tian, *Adv. Funct. Mater.*, 2021, **31**, 2010659.
- 4 P. Pander, A. Swist, J. Soloducho, and F. B. Dias, *Dyes Pigm.*, 2017, **142**, 315-322.
- 5 D. R. Lee, K. H. Lee, W. Shao, C. L. Kim, J. Kim, and J. Y. Lee, *Chem. Mater.*, 2020, **32**, 2583-2592.
- 6 Z. Wang, Y. Zhang, C. Wang, X. Zheng, Y. Zheng, L. Gao, C. Yang, Y. Li, L. and Qu, Y. Zhao, *Adv. Mater.*, 2020, **32**, 1907355.
- 7 L. Xiao, Y. Wu, J. Chen, Z. Yu, Y. Liu, J. Yao, and H. Fu, *J. Phys. Chem. A*, 2017, **121**, 8652-8658.
- 8 Y. Wen, H. Liu, S. Zhang, Y. Gao, Y. Yan, and B. Yang, *J. Mater. Chem. C*, 2019, **7**, 12502-12508.
- 9 Y. Zhou, W. Qin, C. Du, H. Gao, F. Zhu, and G. Liang, *Angew. Chem. Int. Ed.*, 2019, **58**, 12102-12106.
- 10 X. Q. Liu, K. Zhang, J. F. Gao, Y. Z. Chen, C. H. Tung, and L. Z. Wu, *Angew. Chem. Int. Ed.*, 2020, **59**, 23456-23460.
- 11 R. Keruckiene, D. Volyniuk, K. Leitonas, and J. V. Grazulevicius, *Sens. Actuators B Chem.*, 2020, **321**, 128533.
- 12 L. Zang, and H. Zhao, *RSC Adv.* 2020, **10**, 32938-32945.
- 13 Y. Wang, B. Li, Y. Liu, L. Zhang, Q. Zuo, L. Shi, and Z. Su, *Chem. Commun.*, 2009, 5868-5870.
- 14 Z. Xia, N. Xue, W. Shi, and C. Lu, *J. Phys. Chem. C*, 2019, **123**, 30536-30544.